BSim: A System for Three-Dimensional Visualization of Brownian Motion

Technical Report #CS-2006-41

Tenn Francis Chen and Gladimir V. G. Baranoski

Natural Phenomena Simulation Group
School of Computer Science
University of Waterloo
200 University Avenue West
Waterloo, Ontario, Canada N2L 3G1

Abstract

Brownian motion is considered to be of fundamental importance for theoretical and applied scientific research. This report describes an interactive computer graphics system for the three-dimensional visualization of this phenomenon. The system's simulations are based on the formulas provided in Einstein's seminal paper on this topic, which are carefully revisited to introduce the phenomenon's underlying physics. Its predictive capability, which is a key attribute for educational and scientific applications, is demonstrated by the qualitative agreement between simulation results and actual Brownian motion observations.

1 Introduction

Brownian motion, the barely observable but undiminishing movements exhibited by tiny particles suspended in a fluid, is arguably one of the most important scientific phenomena investigated in the last century [21]. As simple as it may seem, the explanation of this motion had a strong impact on the scientific community by supplying concrete physical evidence for the discontinuous nature of matter [21]. Today, Brownian motion continues to trigger ground breaking research in numerous fields from biology to nanotechnology. For example, recent developments involving Brownian motion are providing new insights into fundamental diffusive processes [21].

Since this phenomenon is barely visible to the naked eye, visualizations are often used to assist in the study of its underlying physics. Under most classroom settings, only a top down two-dimensional view of this phenomenon can be seen, however. Furthermore, demonstrations using simple objects (props), such as moving marbles in a tray, do not communicate an accurate physical scale, but only an abstract concept. Therefore, we believe that educational applications aimed at the understanding of Brownian motion can benefit from being able to use interactive three-dimensional systems for its visualization.

Scientific applications can also take advantage of employing such systems. For example, physically-based visualizations can facilitate the observation of subtle geometric patterns which are usually disguised by their complex mathematical representations. The investigation of new theories involving this phenomenon can also be supported by such systems.

This report presents different aspects involved in a three-dimensional physically based visualization of Brownian motion. Initially, it presents an overview of the history and importance of the Brownian motion theory, which is carefully examined. The report then addresses simulation issues and describes a novel system, henceforth referred to as *BSim*, used to simulate and visualize Brownian motion. It closes with a discussion of predictability issues and possible applications.

2 The Phenomenon

2.1 History

Brownian motion was first observed in particles of pollen suspended in water. It remained unexplained and brushed aside as perhaps interesting but unimportant. It appeared to be just a biological phenomenon that had no practical value. When it became apparent that this phenomenon is inorganic, electric and magnetic causes were also suggested [25].

Despite being such an important physical phenomenon, it is actually named after Robert Brown, a well known botanist. Brown is credited, not with discovering Brownian motion, but with realizing that Brownian motion is inorganic. In 1827, he noted that the same "random walk"[1] performed by pollen was also performed by other inorganic particles [21]. A real example of this phenomenon is shown in Figure 1.

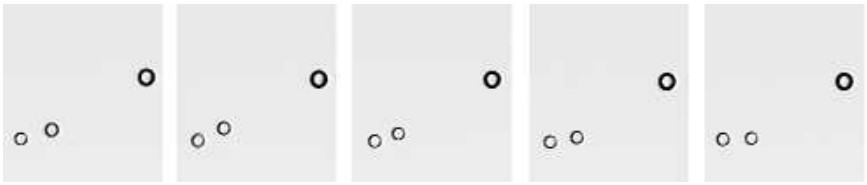

Figure 1: Sequence of microscope images of Brownian motion performed by 1.9 micrometer diameter polystyrene particles suspended in water. The middle particle shows the most noticeable movement throughout these frames. Courtesy of Eric R. Weeks [35].

During the later half of the 19^{th} century, there was an animated rivalry between two parties in the scientific community [21]. This rivalry was caused by paradoxes between the laws of thermodynamics and the kinetic theory (or statistical mechanics). Kinetic theory builds upon the idea that a gas is made up of particles that obey simple laws of Newtonian physics [1]. This states that the motion of the particles can be reversed. However, the second law of thermodynamics states entropy[2] is never decreasing [2]. Therefore, if a gas is really a large collection of particles that obey simple reversible physics, then where does the irreversibility state of entropy come into play?

Shortly after the turn of the century, five papers were published that sent ripples throughout the scientific community [8]. They were neither difficult nor complex, but they approached problems in ways that others neglected. These papers spanned three subject matters: relativity, the photoelectric effect and Brownian motion. These were wondrous papers written by, a then unknown patent clerk, named Einstein.

At that time, there were two established theories about particles in liquids: the hydrodynamic theory[3] and the osmotic theory[4]. Einstein united these two theories. He showed the distance travelled by a particle

[1] A mathematical concept characterized by a sequence of steps where the direction of each step is determined by a random distribution [14].

[2] Entropy can be considered as "order," *i.e.*, the amount of order/chaos is in a system. As an example, an ice cube has smaller entropy (more order) than a volume of water vapour of equal mass [2].

[3] This theory assumes a liquid is a continuous medium which sticks to a solid surface moving through it with not too high a speed [6].

[4] This theory assumes the particle itself a molecule mixed in with a molecular liquid [6].

was proportional to the *square root* of time. This would explain why scientists could not get satisfactory results from measuring the speed of the particles, *i.e.*, distances directly proportional to time.

The theoretical foundations were laid down. However, this paper still did not convince everyone. A French physical chemist, Jean Perrin, took the next step and conducted rigorous experiments [26]. He concluded with empirical results, illustrated in Figure 2, that demonstrated the theoretical predictions of Einstein's paper matched the natural phenomenon, and removed any doubts about Einstein's theory of Brownian motion.

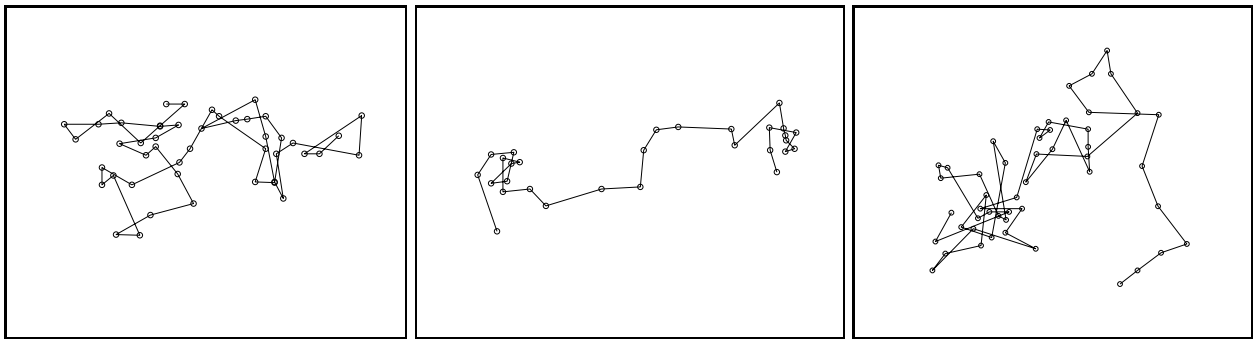

Figure 2: Sketches by Perrin depicting three Brownian motion paths performed by granules of mastic recorded at 30 second intervals. The circles represent the recorded positions of the particles. These figures are redrawn from Nye [26].

2.2 Importance

During the later half of the 19^{th} century, chemists, physicists, and scientists in general were divided into two parties with respect to their belief of what matter really is [21]. One side believed that matter is continuous. They believed the kinetic theory is a convenient tool that can model, but it is not a true physical representation of matter. This was in direct opposition to those who believed matter to be discontinuous, to be made up of many tiny particles.

The immediate result from Brownian motion demonstrated the statistical and discontinuous nature of matter, and unified physicists and chemists under one banner: atoms are real. This little puzzle of a phenomenon, which started out as an anomaly in the microscopes of botanists, revolutionized modern day chemistry and physics and extended to uses in even the stock market [27], population genetics [15] and decision making [30].

2.3 Theory of Brownian Motion

This theory was first presented by Einstein in 1905 [11, 13]. Brownian motion performed by a particle of sand suspended in water occurs because of the tiny movements exhibited by neighbouring water molecules. Consider a ball on a playing field pushed by a great number of people. If this ball is large enough, observing this from a distance would be no different than watching the particle of sand. The people, like the water molecules, cannot be seen because they are too small from this distance, but the motion of the ball is not unlike Brownian motion [16]. The question lies in calculating the displacement: how far does the ball move after a certain period of time?

Einstein combined two theories dealing with particles in liquids: the hydrodynamic theory and the osmotic theory. Since the system is in equilibrium, the osmotic force that pushes particles from high-concentration areas should always balance out with the viscous force that retards this movement.

In the remainder of this section, we revisit Einsetin's original arguments and formulas to provide a clear basis for our Brownian motion simulations. Table 1 summarizes the physical parameters used throughout

Symbol	Definition
D	coefficient of diffusion
E	enthalpy
f	number of particles as a function of position and time
K	osmotic force
k	viscosity of the fluid
N	Avogardo's number
n	total number of particles
n^*	number of particles in V^*
p	osmotic pressure
R	universal gas constant
r	radius of a particle
S	entropy
T	absolute temperature
t	a moment in time
V	total volume
V^*	partition of total volume
v	velocity of a particle
x	a position
Δ	position used for particles' displacement
δp	change in pressure
λ	total root-mean-square displacement of a particle
λ_x	root-mean-square displacement of a particle in x-axis
λ_y	root-mean-square displacement of a particle in y-axis
λ_z	root-mean-square displacement of a particle in z-axis
ν	concentration
τ	time interval passed for displacement to occur
ϕ	weight function

Table 1: Table of symbols used throughout this document.

this document.

2.3.1 Osmotic Force

From the osmotic theory, the osmotic pressure, p, within a partition, V^*, of the total volume, V, is obtained from the ideal gas law [1]:

$$p = \frac{RT}{V^*}\frac{n^*}{N} = \frac{RT}{N}\nu, \tag{1}$$

where R is the universal gas constant, T is the absolute temperature, n^* is number of particles in this partition, N is Avogadro's number and $\nu = \frac{n^*}{V^*}$ is concentration. Using the hydrostatic equation or the second law of thermodynamics (see Appendix), a relationship between the osmotic force, K, and pressure can be obtained:

$$K\nu = \frac{\delta p}{\delta x}. \tag{2}$$

The right side of Equation 2 is the definition of pressure gradient, *i.e.*, the change in pressure, δp, over a distance, δx. Using Equation 1 to replace p in Equation 2 results in:

$$K\nu = \frac{\delta\left(\frac{RT}{N}\nu\right)}{\delta x}. \tag{3}$$

Since R, T, and N are constant within the system, ν is the only value that will change within partitions of the fluid due to the movement of the particles. Therefore, Equation 3 can be rewritten as:

$$\begin{aligned} K\nu &= \frac{RT}{N}\frac{\delta\nu}{\delta x} \\ K &= \frac{RT}{N\nu}\frac{\delta\nu}{\delta x}, \end{aligned} \tag{4}$$

which will be used in the next section.

2.3.2 Osmosis and Viscosity

Assuming the particles are spheres, Stokes's formula[5] can be used to find a relationship between the velocity, v, of a particle and viscosity, k, of the fluid:

$$v = \frac{K}{6\pi kr}, \tag{5}$$

where r is radius of the particle. The number of particles passing through unit area per unit of time due to K is then given by:

$$v\nu = \frac{K\nu}{6\pi kr}. \tag{6}$$

Now, let D be the coefficient of diffusion[6]. The number of particles that will pass through the unit area *due to diffusion* [4] is then given by $D\frac{\delta\nu}{\delta z}$. Since the system is under a dynamic equilibrium, the movement due to K must balance out with movement due to diffusion:

$$\frac{K\nu}{6\pi kr} = D\frac{\delta\nu}{\delta z}. \tag{7}$$

Equation 4 can be used to replace K in Equation 7 to obtain an expression for D:

$$\begin{aligned} \frac{\nu}{6\pi kr}\left(\frac{RT}{N\nu}\frac{\delta\nu}{\delta z}\right) &= D\frac{\delta\nu}{\delta z} \\ D &= \frac{RT}{6\pi kNr}. \end{aligned} \tag{8}$$

2.3.3 Displacement

For simplicity, all motion is assumed to be in one dimension along the x-axis. To actually determine how far a particle moves, let the total number of particles be n. The number of particles that are displaced a distance between Δ and $\Delta + d\Delta$ in time interval τ is given by:

$$dn = n\ \phi(\Delta)d\Delta \tag{9}$$

where weight function $\phi(\Delta)$ is defined by:

$$\int_{-\infty}^{+\infty} \phi(\Delta)d\Delta = 1. \tag{10}$$

To clarify, $\phi(\Delta)d\Delta$ can be viewed as the percentage of particles that experience a displacement between Δ and $\Delta + d\Delta$. As such, dn is a portion of the total number of particles. Also, since a particle has no preference in moving left or right, $\phi(\Delta)$ has a the following property:

$$\phi(\Delta) = \phi(-\Delta). \tag{11}$$

[5] An empirical formula describing the friction experienced by a sphere in a fluid [3].

[6] A proportionality constant that depends on the substance [3].

Let the number of particles per unit volume at position x and time t be $f(x,t)$. The number of particles at time $t+\tau$ between x and $x+dx$ is then given by:

$$f(x,t+\tau)dx = dx\int_{-\infty}^{+\infty} f(x+\Delta,t)\phi(\Delta)d\Delta. \tag{12}$$

The idea is the number of particles at position x at time $t+\tau$ is the number of particles at position $x+\Delta$ that will displace a distance of Δ after τ time. Taylor series[7] can be used to expand $f(x+\Delta,t)$:

$$\begin{aligned} f(x+\Delta,t) = f(x,t) &+ \Delta\frac{\delta f(x,t)}{\delta x} \\ &+ \frac{\Delta^2}{2}\frac{\delta^2 f(x,t)}{\delta x^2} + \dots \end{aligned} \tag{13}$$

Since τ is small, the difference between $f(x,t)$ and $f(x,t+\tau)$ is the rate of change of concentration, $\frac{\delta f}{\delta t}$, multiplied by the time interval τ. This is represented as:

$$f(x,t+\tau) = f(x,t) + \tau\frac{\delta f}{\delta t}. \tag{14}$$

Combining Equations 12, 13 and 14[8] results in:

$$\begin{aligned} f(x,t) + \tau\frac{\delta f}{\delta t} = f&\int_{-\infty}^{+\infty}\phi(\Delta)d\Delta \\ &+ \frac{\delta f}{\delta x}\int_{-\infty}^{+\infty}\Delta\phi(\Delta)d\Delta \\ &+ \frac{\delta^2 f}{\delta x^2}\int_{-\infty}^{+\infty}\frac{\Delta^2}{2}\phi(\Delta)d\Delta + \dots \end{aligned} \tag{15}$$

Taking into account Equation 11, every second term on the right hand side of Equation 15 disappears. We also remark that each remaining term on the right after the third term is very small compared with the previous term. Hence, substituting Equation 10 into Equation 15 gives:

$$\begin{aligned} f + \tau\frac{\delta f}{\delta t} &= f + \frac{\delta^2 f}{\delta x^2}\int_{-\infty}^{+\infty}\frac{\Delta^2}{2}\phi(\Delta)d\Delta \\ \frac{\delta f}{\delta t} &= \left(\frac{1}{\tau}\int_{-\infty}^{+\infty}\frac{\Delta^2}{2}\phi(\Delta)d\Delta\right)\frac{\delta^2 f}{\delta x^2}. \end{aligned} \tag{16}$$

Alternatively, Equation 16 can be written as Fick's second law [4]:

$$\frac{\delta f}{\delta t} = D\frac{\delta^2 f}{\delta x^2}, \tag{17}$$

which is the well known differential equation for diffusion[9] [13]. The solution of Equation 17 is given by [13]:

$$f(x,t) = \frac{n}{\sqrt{4\pi D}}\frac{e^{-\frac{x^2}{4Dt}}}{\sqrt{t}}, \tag{18}$$

[7] $f(x) \doteq \sum_{k=0}^{n}\frac{f^{(k)}(x_0)}{k!}(x-x_0)^k$ [7]

[8] There is a typo in [13] in the Taylor expansion of $f(x,t)+\tau\frac{\delta f}{\delta t}$.

[9] Note that there are now two expressions for D: Equation 8 and $D = \frac{1}{\tau}\int_{-\infty}^{+\infty}\frac{\Delta^2}{2}\phi(\Delta)d\Delta$.

and n can be represented as [13]:

$$n = \int_{-\infty}^{+\infty} f(x,t)dx, \tag{19}$$

which states the total number of particles is the sum of all concentrations over the entire volume. The *root-mean-square displacement*[10] of a particle in the x-axis, λ_x, can be calculated as [22]:

$$\lambda_x = \sqrt{\frac{\int_{-\infty}^{+\infty} f(x,t)x^2dx}{\int_{-\infty}^{+\infty} f(x,t)dx}}. \tag{20}$$

Equations 18 and 19 can be used to replace the numerator and denominator in Equation 20 respectively to obtain:

$$\begin{aligned}
\lambda_x &= \sqrt{\frac{1}{n}\int_{-\infty}^{+\infty}\left(\frac{n}{\sqrt{4\pi D}}\frac{e^{-\frac{x^2}{4Dt}}}{\sqrt{t}}\right)x^2dx} \\
&= \sqrt{\frac{1}{\sqrt{4\pi Dt}}\int_{-\infty}^{+\infty} e^{-\frac{x^2}{4Dt}}x^2dx} \\
&= \sqrt{\frac{1}{\sqrt{4\pi Dt}}\frac{4Dt\sqrt{\pi}}{\frac{1}{\sqrt{Dt}}}} \\
&= \sqrt{2Dt}.
\end{aligned} \tag{21}$$

Finally, replacing D in Equation 21 using Equation 8 results in:

$$\lambda_x = \sqrt{t}\sqrt{\frac{RT}{N}\frac{1}{3\pi kr}}, \tag{22}$$

which is arguably the most quoted outcome of Einstein's first paper on Brownian motion [11, 13].

This one-dimensional result can be extended to three dimensions. The root-mean-square displacement in the y-axis and z-axis, λ_y and $\lambda_z$respectively, are the same as that of the x-axis. Thus, the total root-mean-square displacement, λ, is given by:

$$\begin{aligned}
\lambda &= \sqrt{\lambda_x^2 + \lambda_y^2 + \lambda_z^2} \\
&= \sqrt{3\lambda_x^2} \\
&= \sqrt{t}\sqrt{\frac{RT}{N}\frac{1}{\pi kr}}.
\end{aligned} \tag{23}$$

3 Previous Related Work

Visualizations play an important role in the current scientific community because of its ability to unveil the "invisible." For simple concepts, physical props can be used for illustrative purposes. For instance, stick and ball models can provide a good image of the structure of a small chemical compound. However, when complexity increases, computer graphics becomes an invaluable tool for fulfilling this roll. Furthermore, because of the numerous programming options available, there are many avenues for creating computer graphics visualizations. As an example, Physlets [9] uses Java Applets [18] for the education of physics concepts including Brownian motion.

[10]The root-mean-square is useful when considering the magnitude of a set of oscillating numbers, where the arithmetic mean is zero [22].

Visualization of Brownian motion can be categorized into two types. The first type uses a Newtonian physics model that has smaller fluid particles that bombard and move the larger particle. The second type uses a stochastic method to directly move the solid particles. The Brownian motion simulator within Physlets [9] has an example of the first approach. As an example for the second case, Lipman has created three-dimensional random walk visualizations involving particles colliding with molecular aggregates [24], although the implementation details are not readily disclosed. Han *et al.* [20] also used two dimensional numerical simulations to aid in their investigation of Brownian motion of ellipsoids. This report will concentrate on the latter type of simulations.

To the best of our knowledge, most of the publically available Brownian motion visualizations systems perform only two-dimensional simulation of the phenomenon.

4 Simulation Issues

In this section, practical aspects of our Brownian motion simulator are discussed. The movement of the particles (represented by spheres) and relevant physical parameters are all based upon Einstein's formulation presented in Section 2.3.

4.1 Scale Selection

The selection of appropriate time and space scales is key to obtaining observable simulation results. If a true physical representation is desired, then the core units to be used in the simulation should be small enough to be observed. To illustrate, an object of five meter radius suspended in water at room temperature is not going to exhibit any noticeable Brownian motion in real time. A suitable scale would be to use micrometers in real time. Objects with radius smaller than five micrometers in diameter will demonstrate the phenomena reasonably well.

As an example, assume a room temperature of 20°C and a particle having 5 micrometer radius suspended in water (viscosity of 1.002 cP). After 1 second,

$$\begin{aligned}\lambda &= \sqrt{t}\sqrt{\frac{RT}{N}\frac{1}{\pi kr}} \\ &\doteq \sqrt{1}\sqrt{\frac{8.3144\cdot(273+20)}{6.022\cdot 10^{23}}\frac{1}{\pi\frac{1.002}{1000}\frac{5}{1000000}}} \\ &\doteq 0.51\times 10^{-6}. \end{aligned} \tag{24}$$

This is equivalent to 0.51 micrometers. Although tiny compared to the particle, it is still noticeable compared to the scale of the simulator. This phenomenon will be even more prevalent if the radius of the particle is reduced further.

4.2 Moving Spheres

4.2.1 Choosing a Direction

Since the system is in a pure equilibrium, each particle has equal opportunity to moving in every direction. In three dimensions, there are two degrees of freedom: an azimuthal on the x-y plane and a polar angle with respect to the plane. These angles are labeled as α and β respectively in Figure 3.

To generate these two angles, uniformly generate two variables, u and v, between 0 and 1. Then define the angles as:

$$\begin{aligned}\alpha &= 2\pi u \\ \beta &= \arccos(1-2v).\end{aligned}$$

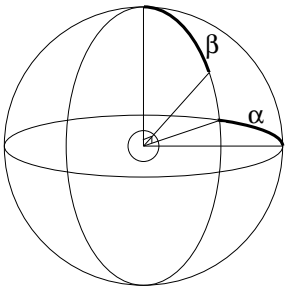

Figure 3: Angles α and β indicate the two degrees of freedom in three dimensions.

4.2.2 Calculating Collision Points

There are two approaches to detect collisions: continuous and discrete [29], which are briefly described below[11].

If objects have a predetermined path to travel on, the exact moment in time when the two objects collide can be calculated. For example, if two spheres following gravity controlled parabolic trajectories are about to collide, the point of intersection can be precisely determined. The trajectories can then be updated and the process repeated. When drawing a frame, the trajectories can be used to calculate the position of the spheres at that moment. This approach is known as continuous.

The discrete approach to detect collisions consists in moving the objects (spheres) at every frame, and determine if the spheres collide at that frame. This is less accurate than the continuous approach. Using the previous example, the spheres may not collide at frame i, but may actually clip at $i + 1$. This is a serious violation of the laws of physics. Furthermore, if the speeds of the objects are high enough, the objects may not be detected as colliding at all, and pass right through each other, *i.e.*, the collision is supposed to occur between frames i and $i + 1$ but the granularity of the frame rate is not fine enough to detect the collision. However, this method is easier to implement in general.

In the described case of simulating Brownian motion, discrete approach can be used, since there is no predetermined path of the particles, and the speeds are relatively slow, *i.e.*, no advantage would be gained by using the first method.

5 *BSim*

The proposed simulator is implemented in C++ [32] using gtkmm [10] and OpenGL [31]. It was originally designed as a simple Newtonian physics simulator of spheres in an enclosed box. All the spheres were assumed to have identical dimensions. It was a simple matter of modifying the physics engine from moving spheres by Newtonian physics to moving the particles using Brownian motion.

5.1 Algorithms

All activity is enclosed by a box and all particles are spheres that share the same physical parameters. A frame is drawn every 20 milliseconds, or 50 frames are drawn per second. At each frame, the state of the system is updated, and a visual representation of the state is drawn to display. There are two main algorithms involved: collision detection and particle movement.

[11] These two approaches are also referred to as *a priori* and *a posteriori* respectively.

5.1.1 Collision Detection

Using the idea mentioned in Section 4.2.2, each particle has its position checked with every other particle at each frame. Since every particle is a sphere, it is easy to test intersections by checking the distance between their centers.

If two particles are clipping, then the two particles are moved away from each other for half of the intersecting distance. For example, let's assume two particles of radius 1.0. If the distance between two particles' centers is 1.0, then, without loss of generality, we move the left particle 0.5 to the left, and the other, 0.5 to the right. This process is shown in Figure 4. A similar process is done with respect to collisions with the walls. However, if a collision occurs, the particle is translated the full distance, and the wall does not move. This inaccuracy is negligible since all movement is stochastic and not pre-determined in any way.

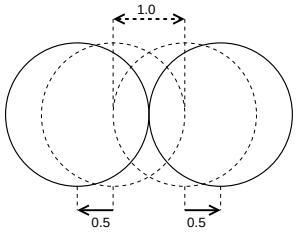

Figure 4: Sketch illustrating the adjustments of clipping spheres. The spheres have a radius of 1.0. The dotted circles represent the unadjusted positions where the centers are 1.0 units apart. The spheres are each moved 0.5 units away from the other sphere to the position of the solid circle, removing the clipping.

5.1.2 Particle Movement

To choose a direction for moving a particle, two random values between 0 and 2π are chosen, one for the azimuthal angle and one for the polar angle, as stated in Section 4.2.

Equation 23 is employed to determine the distance a particle moves. Three physical parameters control the distance a particle moves: the temperature of the system, the viscosity of the fluid, and the radius of the particle. A fourth parameter, the time interval, is set by the frame rate of the graphics system. In this case, the time interval is 20 milliseconds. However, strictly using Equation 23 as displacement is not explicitly accurate since a particle will not always move the distance determined by that expression. As such, the root-mean-square is used as the mean and standard deviation of the Gaussian distribution of the displacement. Gaussian random numbers are generated using the Box-Muller transformation [28].

Since the movement of one particle does not affect the movement of another, the process described above is applied to each particle at every frame.

5.2 User Interface

Figures 5(a) and 5(b) show screenshots of the running program. The current mouse interaction mode is shown at the top and the physical properties shown at the bottom of each screen. The white edges of the bounding volume can be seen behind the spheres, and the jagged path near each sphere is the paths traced by each particle in the last three seconds. These paths are much more obvious in Figure 5(a) than in Figure 5(b). This contrasts the different magnitude of displacement due to the difference in particle radius, illustrating the point mentioned in Section 4.1.

Mouse interaction has two main modes: bounding volume (box) adjustments and camera movements. For the box, this includes scaling the edges, rotating, and translating. For the camera, there are only rotation and translation.

When `Set Properties` is clicked at the bottom right, the input window shown in Figure 6 is displayed. After the properties are set, the simulation continues with these new parameters without resetting.

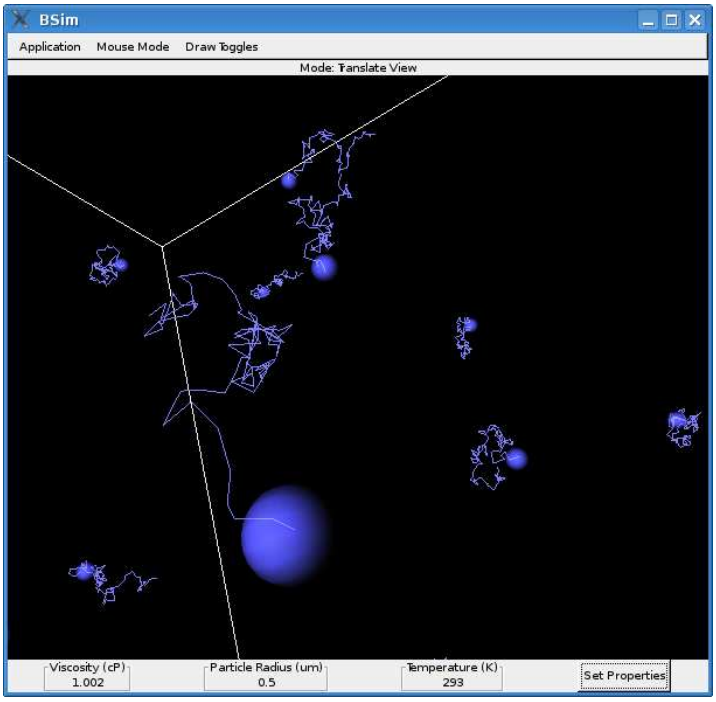

(a)

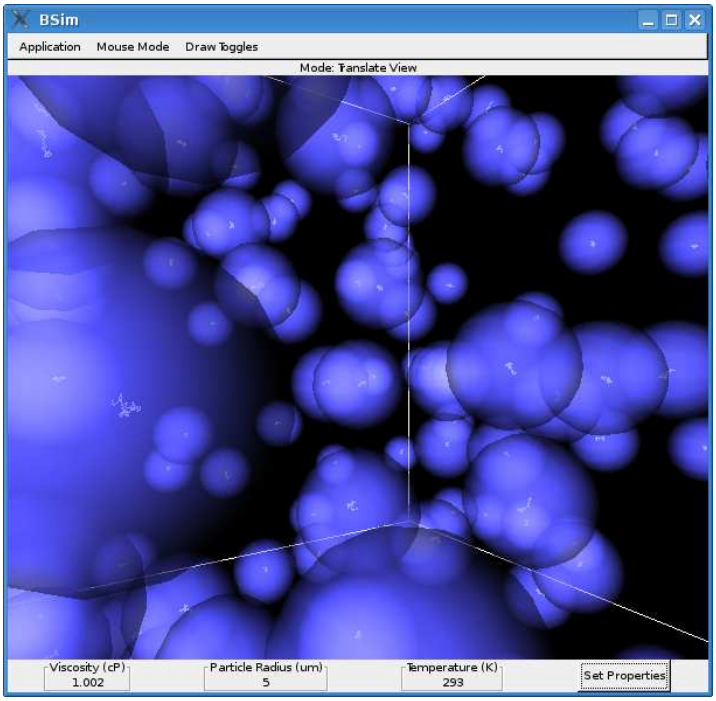

(b)

Figure 5: Screenshots of the running program. (a) Particles with 0.5 micrometer radius. (b) Particles with 5.0 micrometer radius. Jagged lines near each sphere are the paths of the Brownian motion traversed by particles represented by the spheres. Due to the massive size of the particles in Figure 5(b) the jagged lines are reduced to tiny blobs.

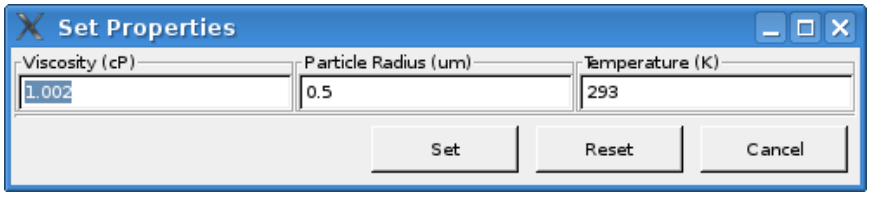

Figure 6: Input dialogue.

Figure 7 shows a sequence of screenshots from *BSim* depicting the development of Brownian motion paths traced by particles in real-time.

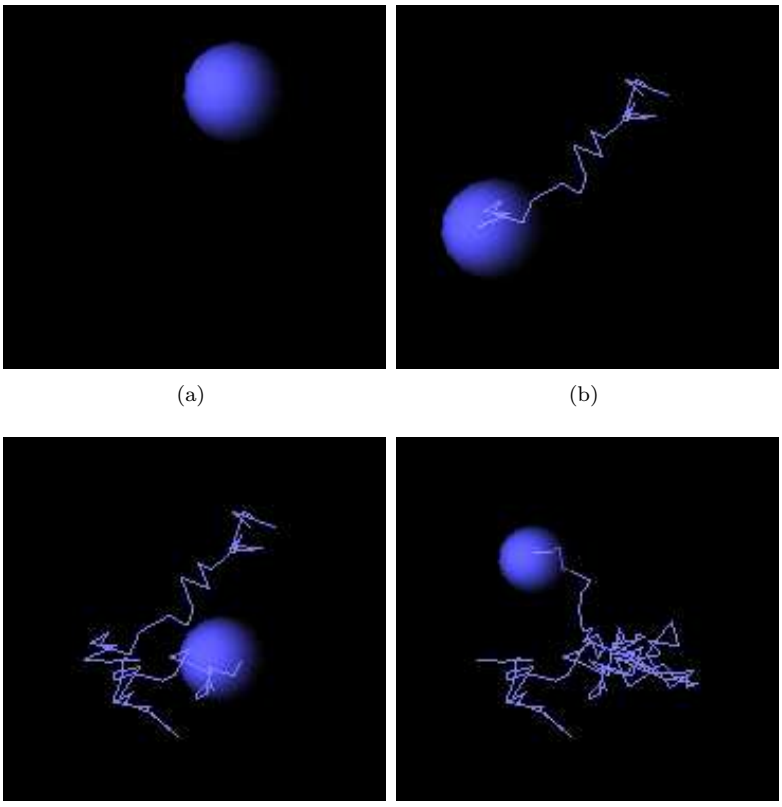

(a) (b)

(c) (d)

Figure 7: This sequence of screenshots from *BSim* show the development of Brownian motion paths (from 7(a) to 7(d)).

5.3 Stereo Capability

The system has the ability to generate simple stereo visualizations using red-blue anaglyphs [33]. It uses the accumulation buffer to overlap two slightly different images. Each image presents a slightly different view of the scene for each eye and red-blue anaglyph glasses are required to filter the scene so each eye only sees one image. A screenshot of *BSim* with the anaglyph option on is shown in Figure 8.

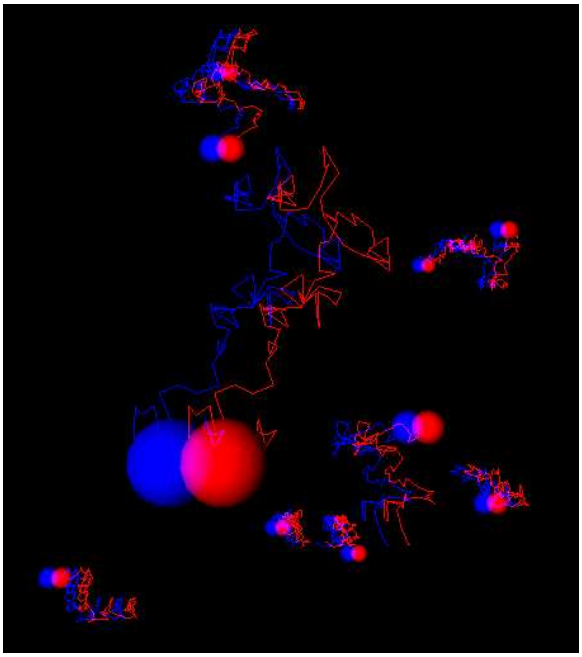

Figure 8: Screenshot of *BSim* with anaglyph enabled.

5.4 Further Improvements

Collision detection can be made more efficient. Currently, every sphere is checked against every other sphere using a naive algorithm, resulting in $O(n^2)$ cost. Collision detection for n objects remains an active area for research [34]. For example, Kim *et al.* [23] have outlined a faster method of detecting collisions. This was not implemented since the initial purpose of the system did not anticipate the need for more than 50 objects.

Using the same underlying physics, the framework can be reworked to a more intensive simulation involving more particles but at the expense of interactivity. Instead of using OpenGL, the framework can be adjusted to use ray casting to create movies of Brownian motion. Currently, depending on the hardware, this simulator can support a few hundred spheres at a time. However, if interactivity is sacrificed, this can turn into a ray casting simulation of thousands or millions of particles that may be applied to other phenomena, *e.g.*, diffusion of dye within a fluid, smoke simulations and even the visualization of plasma manifestations [5].

6 Predictability

For a visual simulation of a physical phenomenon to be considered *predictable*, it needs to be controlled by physically meaningful parameters, take into account the underlying physical processes and be able to provide scientifically sound results [19]. The last aspect should be verified through quantitative and qualitative comparisons with actual observations of the phenomenon. In the case of *BSim*, the stochastic nature of Brownian does not favor quantitative comparisons between simulated results and actual observations of the phenomenon. Nevertheless, it is possible to perform qualitative comparisons with experimental data provided in the literature. Figure 9 shows three plots of data generated by *BSim*. These results show a good qualitative agreement with Perrin's original sketches of Brownian motion paths performed by granules of mastic shown in Figure 2.

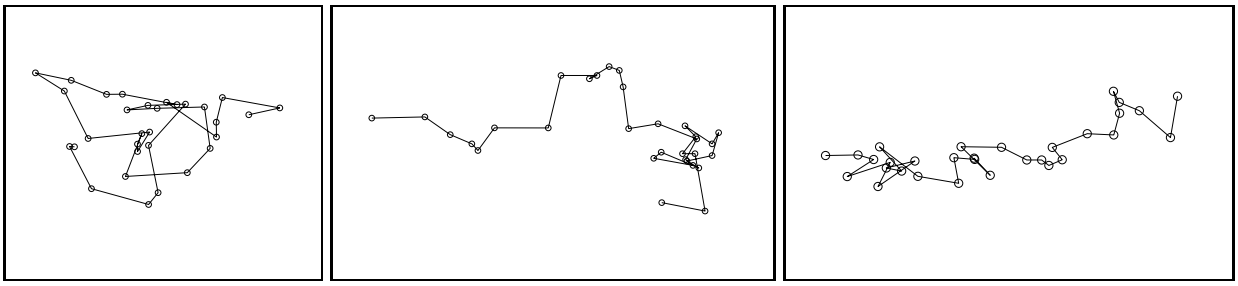

Figure 9: Plot of x and y coordinates of three Brownian motion paths generated by *BSim*. The circles represent the positions of the modeled particles.

7 Concluding Remarks

This report has revisited Einstein's theory of Brownian motion, and presented a simulator that uses the physics derived from this seminal work. The physics described here can be used as a basis for other visualization platforms that share this common physical core. The proposed simulator, *BSim*, gives an accurate scale of the actual phenomenon, and it allows the observation of how different parameters affect the magnitude of Brownian motion. As such, we believe that *BSim* can be a useful too in educational applications and investigations of particle based processes such as visual manifestations of plasma phenomena.

Future developments for *BSim* can include parallelism and rotation of particles. The independence of each particle allows each step of the random walk to be simultaneously calculated using multiple processing units. This increase in computing power will allow us to employ a larger number of particles, as well as introduce other details of the phenomenon. Currently, the system only simulates the displacement of the particles. Einstein's second paper on this topic [12] introduces particle rotation which would be a natural extension of this project in the future.

References

[1] Alonso, M., and Finn, E. J. *Fundamental University Physics*, second ed., vol. 1: Mechanics and Thermodynamics. Addison-Wesley Publishing Company, 1980, pp. 412–420.

[2] Alonso, M., and Finn, E. J. *Fundamental University Physics*, second ed., vol. 1: Mechanics and Thermodynamics. Addison-Wesley Publishing Company, 1980, pp. 450–453.

[3] Alonso, M., and Finn, E. J. *Fundamental University Physics*, second ed., vol. 1: Mechanics and Thermodynamics. Addison-Wesley Publishing Company, 1980, p. 157.

[4] Alonso, M., and Finn, E. J. *Fundamental University Physics*, second ed., vol. 1: Mechanics and Thermodynamics. Addison-Wesley Publishing Company, 1980, pp. 464–471.

[5] Baranoski, G. V. G., and Rokne, J. G. Rendering plasma phenomena: Applications and challenges. In *Proceedings of the State of the Art Reports of EUROGRAPHICS 2006* (2006), pp. 63–88.

[6] Brush, S. G. A history of random processes, I. Brownian movement from Brown to Perrin. *Archive for History of Exact Sciences 5* (1968), 1–36.

[7] Burden, R. L., and Faires, J. D. *Numerical Analysis*, fifth ed. PWS Publishing Company, 1993, p. 8.

[8] Chalmers, M. Five papers that shook the world. *Physics World 18*, 1 (2005), 16–17.

[9] Christian, W., and Belloni, M. *Physlets: Teaching Physics with Interactive Curricular Material*. Prentice Hall, 2000.

[10] Cumming, M., Rieder, B., Jongsma, J., M'Sadoques, J., Laursen, O., Gustin, C., and Anastasov, M. Programming with gtkmm, 2002-2006. Available at: http://www.gtkmm.org/docs/gtkmm-2.4/docs/tutorial/html/index.html.

[11] Einstein, A. Über die von der molekularkinetischen theorie der wärme geforderte bewegung von in ruhenden flüssigkeiten suspendierten teilchen. *Annalen der Physik 17* (1905), 549–560.

[12] Einstein, A. Zur theorie der brownschen bewegung. *Annalen der Physik 19* (1906), 371–381.

[13] Einstein, A. *Investigations on the Theory of Brownian Movement*. Dover Publications, Inc., 1956. Translated by A. D. Cowper.

[14] Feller, W. *An Introduction to Probability Theory and its Applications*, vol. 1. John Wiley & Sons, Inc., 1950, ch. 14.

[15] Feng, S., and Hoppe, F. M. Large deviation principles for some random combinatorial structures in population genetics and brownian motion. *Annals of Applied Probability 8*, 4 (1998), 975–994.

[16] Feynman, R. P. *Feynman Lectures On Physics*, vol. 1. Addison Wesley Longman, 1970, ch. 41.

[17] Feynman, R. P. *Feynman Lectures On Physics*, vol. 2. Addison Wesley Longman, 1970, ch. 40.

[18] Flanagan, D. *Java in a Nutshell*, fifth ed. O'Reilly & Associates, 2005.

[19] Greenberg, D. P., Torrance, K. E., Shirley, P., Arvo, J., Lafortune, E., Ferwerda, J. A., Walter, B., Trumbore, B., Pattanaik, S., and Foo, S.-C. A framework for realistic image synthesis. In *SIGGRAPH '97: Proceedings of the 24th annual conference on Computer graphics and interactive techniques* (Aug. 1997), pp. 477–494.

[20] Han, Y., Alsayed, A. M., Nobili, M., Zhang, J., Lubensky, T. C., and Yodh, A. G. Brownian motion of an ellipsoid. *Science 314*, 5799 (2006), 626–630.

[21] Haw, M. Einstein's random walk. *Physics World 18*, 1 (2005), 19–22.

[22] Kenney, J. F., and Keeping, E. S. *Mathematics of Statistics, Part 1*, third ed. D. Van Nostrand Company, Inc., 1954, ch. 4.15.

[23] Kim, D.-J., Guibas, L. J., and Shin, S.-Y. Fast collision detection among multiple moving spheres. *IEEE Transactions on Visualization and Computer Graphics 4*, 3 (1998), 230–242.

[24] Lipman, R. Random walk visualization, 2000. Further information can be found at: http://cic.nist.gov/lipman/sciviz/random.html.

[25] Nye, M. J. *Molecular Reality*. American Elsevier Publishing Company, Inc., 1972, pp. 9–29.

[26] Nye, M. J. *Molecular Reality*. American Elsevier Publishing Company, Inc., 1972, pp. 126–136.

[27] Osborne, M. F. M. Brownian motion in the stock market. *Operations Research 7*, 2 (1959), 145–173.

[28] Press, W. H., Teukolsky, S. A., Vetterling, W. T., and Flannery, B. P. *Numerical recipes in C (2nd ed.): the art of scientific computing*. Cambridge University Press, New York, NY, USA, 1992.

[29] Redon, S., Kheddar, A., and Coquillart, S. Fast continuous collision detection between rigid bodies. In *Computer Graphics Forum* (Sept. 2002).

[30] Romanow, A. L. A Brownian motion model for decision making. *Journal of Mathematical Sociology 10* (1984), 1–28.

[31] Shreiner, D., Woo, M., Neider, J., and Davis, T. *OpenGL Programming Guide: The Official Guide to Learning OpenGL, Version 2*, fifth ed. Addison-Wesley Professional, 2005.

[32] Stroustrup, B. *The C++ Programming Language*, third ed. Addison-Wesley Professional, 1997.

[33] Waack, F. G. *Stereo Photography.* The Stereoscopic Society, 1985.

[34] Watt, A., and Policarpo, F. *3D Games: Real-time Rendering and Software Technology*, vol. 1. Addison-Wesley, 2001.

[35] Weeks, E. R. Introduction to random walks and Brownian motion. Available at: http://www.physics.emory.edu/ weeks/squishy/BrownianMotion.html.

Appendix
Osmotic Pressure and Force

There are two ways to derive the relationship between osmotic pressure and force. Einstein used the second law of thermal dynamics [11], while Fürth suggested to directly use the equation that relates force to pressure [13]. The two different approaches are outlined below.

1. Using the second law of thermal dynamics, the change of free energy of an isothermal system can be written as:
$$\delta F = \delta E - T\delta S = 0, \tag{25}$$
where δE is the change in enthalpy, T is the temperature and δS is the change in entropy. This equation is also known as Gibbs Free Energy.

   Now,
$$\delta E = -\int_0^1 K\nu\delta x dx \tag{26}$$
   and
$$\begin{aligned}\delta S &= \int_0^1 R\frac{\nu}{N}\frac{\partial\delta x}{\partial x}dx \\ &= -\int_0^1 \frac{R}{N}\frac{\partial\nu}{\partial x}\delta x dx.\end{aligned} \tag{27}$$
   Then, substituting Equations 26 and 27 into Equation 25 yields:
$$\begin{aligned}-\int_0^1 K\nu\delta x dx - T\left(-\int_0^1 \frac{R}{N}\frac{\partial\nu}{\partial x}\delta x dx\right) = 0 \\ \int_0^1 \left(-K\nu + \frac{RT}{N}\frac{\partial\nu}{\partial x}\right)\delta x dx = 0.\end{aligned} \tag{28}$$
   Thus,
$$K\nu = \frac{RT}{N}\frac{\partial\nu}{\partial x} = \frac{\partial p}{\partial x}. \tag{29}$$

2. The second approach is to use the hydrostatic equation [17]:

$$\partial p = -g\rho\partial h, \tag{30}$$

where ∂p is the change in pressure, $-g$ is the acceleration due to gravity, ρ is the density in $\frac{kg}{m^3}$ and ∂h is the change in height. This equation is frequently used in meteorology to explain the pressure differences in the atmosphere. This equation can be modified so that gravity times density, $-g\rho$, is replaced by force times concentration, $K\nu$, and instead of change in height, ∂h, change in distance, ∂x, is used:

$$\begin{aligned} \partial p &= K\nu\partial x \\ \frac{\partial p}{\partial x} &= K\nu. \end{aligned} \tag{31}$$

For more details about these two approaches, the reader is directed to Brush [6], Einstein's paper [11] and the notes in the translation of Einstein's paper [13].